Variable Sodium on the Surface of Mercury: Implications for Surface Chemistry and the Exosphere. Larry G. Evans[1], Patrick N. Peplowski[2], Rosemary M. Killen[3], Andrew E. Potter[4], Ann L. Sprague[5], [1]Computer Science Corporation, Lanham-Seabrook, MD 20706, USA (Larry.G.Evans@nasa.gov); [2]The Johns Hopkins University Applied Physics Laboratory, Laurel, MD 20723, USA; [3]NASA Goddard Space Flight Center, Greenbelt, MD 20771, USA; [4]National Solar Observatory, Tucson, AZ, USA 85719, [5]University of Arizona, Tucson, AZ 85719, USA.

Introduction: The nature and origin of volatile elements on the surface of Mercury have long been outstanding questions. The majority of the formation mechanisms proposed for Mercury predict that the present-day surface should be volatile depleted [1]. These predictions contrast with terrestrial and space-based observations of Mercury's exosphere that have identified the moderately volatile species K [2] and Na [3]. The MESSENGER spacecraft carries an extensive payload of scientific instruments designed in part to examine volatile elements on the surface and in the exosphere [4]. Orbital measurements of the surface composition made by the X-Ray Spectrometer (XRS) [5] and Gamma-Ray Spectrometer (GRS) [6] have led to the discovery of relatively high surface abundances of the volatile elements S [7, 8], K [9], and Na [8]. We report evidence for spatial variations in the abundance of Na on Mercury's surface and their relation to latitudinal variations in Mercury's Na exosphere.

Gamma-Ray Measurements: Previous observations of Na were limited to a single measurement of the average abundance (2.9 ± 0.1 wt%) in the northern hemisphere [8]. This limitation stems from the highly eccentric orbit of MESSENGER about Mercury coupled with the altitude-dependence of the gamma-ray signal. The Na abundance [8] was found to be consistent with terrestrial mid-infrared observations suggestive of the presence of Na-bearing plagioclase feldspar [11]. Petrologic modeling of the composition of Mercury's crust from the surface elemental compositions [8, 12] indicates that a substantial abundance of Na-rich plagioclase (as much as 57%) is possible in the northern volcanic plains units [13].

In order to relate Na exosphere measurements to the GRS results, it is necessary to map the latitudinal variation of the Na abundance. A new analysis of the Na peak has been performed using only low-altitude, southbound data in order to maximize the spatial resolution of the measurements. Unfortunately, this restriction has a negative effect on the statistical significance of the measurements.

The Na/Si mass ratio is plotted against latitude along with one-standard-deviation (σ) errors in Figs. 1 and 2. The northernmost Na/Si value is found to be significantly (3.5σ) higher (0.17 ± 0.02) than the average equatorial value (~0.10). When coupled with the known homogeneity of Si over the same region [10], this is evidence for variable Na abundance over the surface of Mercury.

Interpretation: We propose two hypotheses to account for the observed Na/Si abundance distribution. Under the first hypothesis, the high-reflectance smooth plains (SP) units are assumed to have a Na composition that differs from that of the older surrounding intercrater plains and heavily cratered terrain (IcP/HCT). Distinct Na/Si abundance ratios were assigned to the SP and IcP/HCT, and the resulting gamma-ray signals were modeled and forward propagated to the spacecraft given the known distribution of the two terrain types [14]. Fig. 1 compares these predictions, summed by latitude, to the GRS measurements. The comparison shows that this hypothesis is consistent with the data for Na abundances of 3.9−5.2 wt.% in the SP and 0.7−2.9 wt.% for the IcP/HCT areas (for a Si abundance of 24.6 wt%; see [8]). The endpoints of these ranges correspond to the colored curves in Fig. 1.

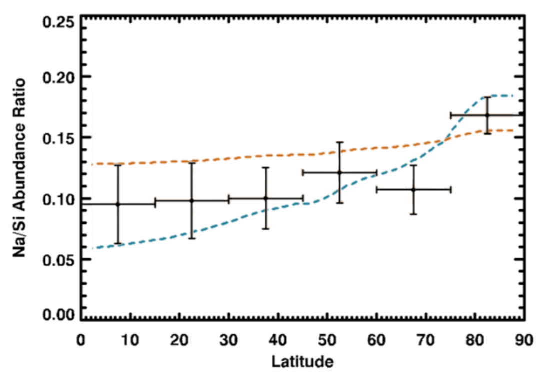

Figure 1. Na/Si abundances and one-standard-deviation statistical uncertainties as measured by the MESSENGER Gamma-Ray Spectrometer, plotted as a function of latitude. Forward models of Na/Si abundance distribution for two models in which the smooth plains have higher Na/Si values than surrounding terrain are shown as dashed lines. The orange line corresponds to values of 0.16 and 0.12 and blue line to values of 0.21 and 0.03 for the SP and IcP/HCT, respectively.

A second hypothesis is that Na has been thermally mobilized on the surface, and the result is higher Na in cooler polar regions. This hypothesis, earlier motivated by ground-based studies of the Na exosphere [9], follows from a similar interpretation of the spatial distribution for K on Mercury [10]. From maps of maximum surface temperature and assuming a similar temperature dependence for Na as that seen for K, Na/Si abundances were assigned and the resulting gamma-ray fluxes were modeled and compared with GRS measurements (Fig. 2). This model is also consistent with the data, with allowed Na abundances of 3.7−4.7 wt.% in the cooler regions and 1.5−3.2 wt.% in the warmer equatorial regions. The endpoints of these ranges correspond to the colored curves in Fig. 2.

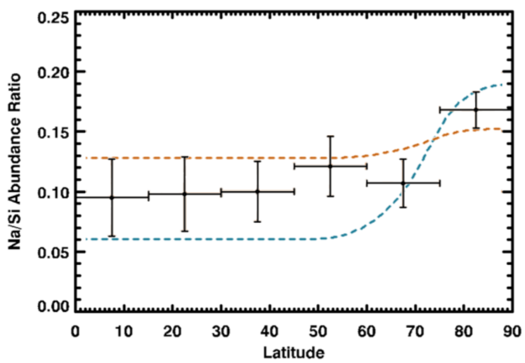

Figure 2. Na/Si abundance as measured by the MESSENGER Gamma-Ray Spectrometer, plotted as a function of latitude. Forward models of an assumed Na/Si abundance that varies as the maximum surface temperature are shown as dashed lines. The orange line corresponds to values of 0.15 and 0.13 and blue line to values of 0.19 and 0.06 in the polar and non-polar regions, respectively.

Exosphere Observations: It has long been observed that the spatial distribution of Na in Mercury's exosphere, although variable, often exhibits enhancements at one or both poles. Taking advantage of a rare opportunity to observe the transit of Mercury across the face of the Sun, measurements on 8 November 2006 (Fig. 3) show that the exospheric density was clearly enhanced at both poles, with the extent of the enhancement wider in the south, consistent with a larger cusp region in the south [15].

The temperatures of the atoms inferred by the transit (750–1500 K near the poles, and 1500–3000 K in equatorial regions) are consistent with those inferred from high-spectral-resolution observations, about 750 K over the poles and 1200 K in the equatorial regions [16]. MESSENGER MASCS observations also indicate a Na temperature of 1200 K at the equator near the surface. These observations are broadly consistent with those taken during the transit of 2003 [17]. There is no statistical difference between the northern and southern portions of the Na tail seen during the first and second MESSENGER flybys [18].

Ground-based observations often show enhancements at high latitudes, varying on time scales of hours [e.g., 19, 20]. For example, the exosphere was enhanced in the southern hemisphere on 15 January 2008 [19]. The K exosphere shows similar high-latitude enhancements [21]. Such high-latitude enhancements could be consistent with a higher intrinsic abundance at high latitudes, along with ion-enhanced desorption in the polar cusp regions. There is not a one-to-one correspondence between the surface abundance and the exosphere at all times, but temporal variations indicate a complex interaction between the surface abundance and the source processes.

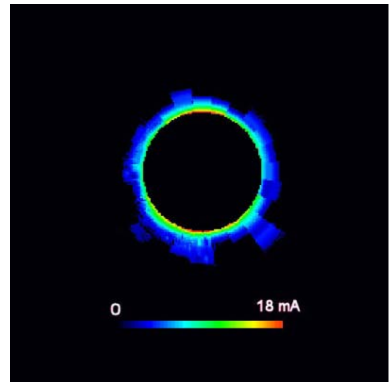

Figure 3. The Na exosphere at the limb observed from the Dunn solar telescope at Sunspot, NM, on 8 November 2006 (Potter et al. 2013), shows enhanced density at both poles, with equivalent width shown in milli-Angstroms.

Monte-Carlo modeling of MASCS data, using the underlying Na abundance observed by the GRS and estimates of solar wind flux, are currently underway in an effort to further constrain the relationship between the surface and exospheric abundances.

References: [1] Taylor, J.J. and Scott, E.R.D. (2003), *Treatise on Geochemistry*, Vol. 1, pp. 477−485, Elsevier. [2] Potter, A.E. and T.H. Morgan (1986) *Icarus 67*, 336−340. [3] Potter, A.E. and T.H. Morgan (1985) *Science 229*, 651−653. [4] Solomon, S.C. et al. (2007) *Space Sci. Rev. 131*, 3−39. [5] Schlemm, C.E., II, et al. (2007) *Space Sci. Rev. 131*, 393−415. [6] Goldsten, J.O. et al. (2007) *Space Sci. Rev. 131*, 339−391. [7] Nittler, L.R. et al. (2011) *Science 333*, 1847−1850. [8] Evans, L.G. et al. (2012) *JGR 117*, E00L07. [9] Domingue, D.L. et al. (2007) Space Sci. Rev., 131, 161−186. [10] Peplowski, P.N. et al. (2012) *JGR 117*, E00L04. [11] Sprague, A.L. et al. (2007) *Space Sci. Rev. 132*, 399−431. [12] Weider, S.Z. et al. (2012) *JGR 117*, E00L05. [13] Stockstill-Cahill, K.R. et al. (2012), *JGR 117*, E00L15. [14] Denevi, B.W. et al. (2012) *JGR*, submitted. [15] Potter, A.E. et al. (2013) Icarus, submitted. [16] Killen, R.M. et al. (1999) Planet. Space Sci., 47, 1449-1458. [17] Schleicher, H. et al. (2004) Astron. Astrophys. 425, 1119−1124. [18] Burger, M.H. et al. (2010) Icarus 209, 63−74. [19] Mouawad, N. et al. (2011) Icarus, 211, 21−36. [20] Mangano, V. et al. (2012) eprint arXiv:1209.47682012. [21] Killen, R.M. et al. (2010) Icarus, 209, 75−78.